

To appear in the *International Journal of Control*  
Vol. 00, No. 00, Month 20XX, 1–23

## Model orbit output feedback tracking of underactuated mechanical systems with actuator dynamics

LEONARDO HERRERA<sup>a</sup>, YURY ORLOV<sup>a</sup>, OSCAR MONTANO<sup>a</sup> AND ANTON SHIRIAEV<sup>b</sup>

<sup>a</sup> Department of Electronics and Telecommunications, Center for Scientific Research and Higher Education  
at Ensenada, Baja California,  
Carretera Ensenada-Tijuana No. 3918, Zona Playitas, C.P. 22860, Ensenada, B.C., Mexico.

<sup>b</sup> Department of Engineering Cybernetics, Norwegian University of Science and Technology,  
7491 Trondheim, Norway.

[xxxx]

(Received 00 Month 20XX; accepted 00 Month 20XX)

Robust periodic motion generation is developed for a class of mechanical systems with actuator dynamics. The virtual constraint (VC) approach is first refined under incomplete state measurements and it is then extended to the case where the actuator dynamics are brought into play for avoiding limitations in the system performance. The extended virtual constraint approach is subsequently coupled to the nonlinear  $\mathcal{H}_\infty$  synthesis to yield the robust output feedback periodic motion generation for mechanical systems of underactuation degree one, driven by electrical motors with their own dynamics. The effectiveness of the proposed synthesis is supported in the numerical study made for a cart-pendulum testbed.

**Keywords:** robust control, mechanical systems, orbital stabilization, disturbance attenuation, actuator dynamics.

## 1. Introduction

Professor Alexander Fradkov has contributed with the rich legacy Fomin, Fradkov & Yakubovich (1981); Fradkov *et al.* (1999) in the adaptive control area. Model reference adaptive control (MRAC) design is well-recognized in the modern automatic control engineering for reproducing desired dynamics in spite of the deficit of the knowledge of the plant parameters. Being extended by Orlov *et al.* (2005) to model orbit robust stabilization (MORS) of Pendubot, the utility of the MRAC approach was additionally demonstrated for the periodic motion generation under uncertain plant parameters. In the present paper, the MORS design is generalized for underactuated mechanical systems, driven by electrical motors with their own dynamics. The proposed generalization invokes the virtual constraint (VC) approach Shiriaev *et al.* (2005) for designing a feasible orbit model to subsequently include it into the nonlinear  $\mathcal{H}_\infty$  output feedback synthesis of underactuated mechanical systems, augmented with actuator dynamics.

The VC approach is a powerful tool of the periodic motion generation in underactuated mechanical systems such as pendulum and biped robots. Its practical utility is well-established for a particular case of underactuation degree one (see, e.g., the references Chevallereau *et al.* (2013); Freidovich *et al.* (2008); Shiriaev *et al.* (2008); Westervelt *et al.* (2007) to name a few). Potential generalizations to multi degrees of underactuation are of higher complexity and are presently confined to specific applications, mainly of underactuation degree two Shiriaev *et al.* (2010). The periodic motion generation under incomplete and imperfect state measurements is another challenge in the use of the VC approach that has not yet been addressed in the literature.

The applicability of the VC approach, typically relying on the state feedback transformation, is constructively extended to the periodic motion generation in underactuated mechanical systems with actuator dynamics when only incomplete noise-corrupted state measurements are available. For transparency, the output feedback exposition is confined to mechanical systems of the underactuation degree one, however, extension to higher underactuation degrees is indeed possible whenever the VC proves to be applicable to the state feedback design where the actuator dynamics are ignored.

Within the standard state feedback framework, the VC approach is first utilized to design a reference model, possessing an asymptotically stable limit cycle. Once such a reference model is constructed, it is involved into the nonlinear  $\mathcal{H}_\infty$  output feedback model tracking, inspired from Brogliato *et al.* (2007); Isidori & Astolfi (1992); Orlov & Aguilar (2014); Ortega *et al.* (2013), to yield the robust generation of the periodic motion in the underlying system with imperfect partial state measurements. The resulting synthesis procedure is thus applicable under noise-corrupted partial state measurements, thereby refining the VC approach.

The developed procedure is additionally extended to underactuated mechanical systems, driven by electrical motors with their own linear dynamics of the first order. The over-all plant-actuator dynamics are thus no longer in the Lagrangian form. Although controlling mechanical manipulators with actuator dynamics has been addressed in the literature, e.g., in Chen *et al.* (1998); Moon *et al.* (1997); Wang *et al.* (2009), however, it has been confined to fully actuated mechanical systems with complete information on the state vector. The present development deals with mechanical systems of the underactuation degree one, whose synthesis involves actuator dynamics and incomplete and imperfect measurements, and therefore it becomes of higher complexity due to the absence of the information on the actuator state and due to the need of the construction of additional transversal coordinates, corresponding to the actuator dynamics.

Thus, the paper contributes to the existing literature by presenting the robust procedure of the periodic motion generation which is viable for a broad class of electromechanical systems of the underactuation degree one with actuator dynamics and with partial state measurements. Capabilities of the proposed periodic motion generation and its robustness features are supported in the numerical study of a cart-pendulum benchmark model, driven by an electrical motor.

The rest of the paper is outlined as follows. In Section 2, a generic electromechanical system

of interest is introduced and the robust synthesis procedure is developed for the periodic motion generation in the underlying system. The attractive features of the proposed synthesis are then illustrated in Section 3, where the developed procedure is applied to a benchmark emulator of underactuation degree one, driven by an electrical motor. Finally, Section 4 collects some conclusions.

## 2. Objective and Control Strategy

The primary concern of the present investigation is to achieve a periodic motion stabilization of a mechanical system of underactuation degree one, driven by electrical motors with their own dynamics and operated under uncertainty conditions such as external disturbances and imperfect partial state measurements. A mathematical model for such a system is given by

$$M(q)\ddot{q} + C(q, \dot{q})\dot{q} + G(q) = B\tau + w_q. \quad (1)$$

whereas the actuator dynamics  $\tau$  are governed by

$$\dot{\tau} = -A_\tau\tau + B_\tau\nu + w_\tau. \quad (2)$$

In the above relations, the vectors  $q \in \mathbb{R}^n$  and  $\dot{q} \in \mathbb{R}^n$  are generalized positions and velocities, respectively,  $\tau \in \mathbb{R}^{n-1}$  is the vector of actuated torques, which are driven by the corresponding voltage components of the input vector  $\nu \in \mathbb{R}^{n-1}$ . From the physical point of view,  $M \in \mathbb{R}^{n \times n}$  is an inertia matrix, which is positive definite and continuously differentiable,  $C(q, \dot{q}) \in \mathbb{R}^n$  stands for centrifugal and Coriolis forces,  $G(q)$  is for the gravity forces; in the classical analytical mechanics,  $M, C, G$  are represented by smooth functions. The constant matrix  $B \in \mathbb{R}^{n \times (n-1)}$  of rank  $n-1$  is composed of 0 and 1 to specify the underactuated variables and actuated ones,  $A_\tau, B_\tau$  are nonsingular diagonal matrices of the appropriate dimensions, which determine the linear behavior of the actuator dynamics. The  $n$ -vector function  $w_q(\cdot) \in \mathbb{R}^n$  and  $(n-1)$ -vector function  $w_\tau$  are deliberately involved into modeling to account for external plant disturbances and, respectively, for actuator disturbances as well as for model inadequacies. Throughout, these functions are assumed to be square integrable on any finite time interval and their influence on the closed-loop behavior should locally be attenuated. The corresponding disturbance attenuation problem is properly stated and solved in Section 2.2 based on the well-known nonlinear  $\mathcal{H}_\infty$  approach.

Research interest to the orbital stabilization of mechanical systems is inspired from applications where the natural operation mode is periodic. The control objective for the orbital stabilization (e.g., periodic trajectory planning for industrial robot manipulators Chevallereau *et al.* (2013)) is typically to generate a closed-loop system that possesses its own limit cycle in the absence of external disturbances and measurement errors, while also attenuating their effect, otherwise. In the sequel, the VC approach serves as an instrumental tool which allows one to design an appropriate reference model with an asymptotically stable limit cycle. The desired orbitally stabilizing synthesis is then composed of the nonlinear  $\mathcal{H}_\infty$  output feedback controller that tracks the reference model thus constructed. The resulting synthesis procedure constitutes a new orbital stabilization paradigm under noise-corrupted partial state measurements and it is specified below for mechanical systems of underactuation degree one, augmented with actuator dynamics.

### 2.1 Reference model design

At the first step, the VC approach of Shiriaev *et al.* (2005) is extended to a disturbance-free copy

$$M(q^*)\ddot{q}^* + C(q^*, \dot{q}^*)\dot{q}^* + G(q^*) = B\tau^* \quad (3)$$

$$\dot{\tau}^* = -A_\tau\tau^* + B_\tau\nu^* \quad (4)$$

of the generic plant-actuator system (1), (2) to design a reference input

$$\nu^* = F(q^*, \dot{q}^*, \tau^*) \quad (5)$$

such that the closed-loop system (3), (4), (5) possesses an asymptotically stable limit cycle. For this purpose, a virtual geometric (i.e., holonomic) constraint

$$q_1^* = r_1(\phi), \dots, q_n^* = r_n(\phi), \quad (6)$$

where  $r_i(\phi)$ ,  $i = 1, \dots, n$  are smooth functions of a parameter  $\phi$ , is found in accordance with Shiriaev *et al.* (2005) to achieve an alternative representation of the motion. Frequently, one of the coordinates, say  $q_n^*$  for certainty, is a good choice of the parameter  $\phi$  with  $r_n(\phi) = \phi$ . The reference input design strategy is thus to ensure that manifold (6) is attractive for the closed-loop system (3)-(5).

The quantities

$$\phi, \zeta_1 = q_1^* - r_1(\phi), \dots, \zeta_n = q_n^* - r_n(\phi). \quad (7)$$

yield excessive coordinates, one of which, e.g.,  $\zeta_n$  can be viewed as a function of others. Thus, the variables

$$\zeta = (\zeta_1, \dots, \zeta_{n-1})^T \in \mathbf{R}^{n-1} \text{ and } \phi \in \mathbf{R} \quad (8)$$

determine new independent coordinates where the vector  $\zeta$  is transversal to the virtual manifold (6). In terms of these coordinates, the plant dynamics can be represented in the form Shiriaev *et al.* (2005)

$$\ddot{\zeta} = R(\zeta, \dot{\zeta}, \phi, \dot{\phi}) + N(\zeta, \phi)\tau^*, \quad (9)$$

$$\alpha(\phi)\ddot{\phi} + \beta(\phi)\dot{\phi}^2 + \gamma(\phi) = \mu(\zeta, \dot{\zeta}, \phi, \dot{\phi}, \ddot{\phi}, \tau^*) \quad (10)$$

where  $R, N, \alpha, \beta, \gamma, \mu$  are smooth vector functions of appropriate dimensions.

It is worth noticing that the function  $\mu$  in (10) is linear in  $\tau^*$  and it is nullified for  $\zeta = \dot{\zeta} = 0$ , i.e.,

$$\mu(\zeta, \dot{\zeta}, \phi, \dot{\phi}, \tau^*) = \mu_1(\zeta, \dot{\zeta}, \phi, \dot{\phi}, \ddot{\phi})\zeta + \mu_2(\zeta, \dot{\zeta}, \phi, \dot{\phi}, \ddot{\phi})\dot{\zeta} + \mu_3(\zeta, \dot{\zeta}, \phi, \dot{\phi}, \ddot{\phi})\tau^* \quad (11)$$

with appropriate functions  $\mu_1, \mu_2, \mu_3$  such that  $\mu_3(0, 0, \phi, \dot{\phi}, \ddot{\phi}) = 0$ . Thus, (10) degenerates to

$$\alpha(\phi)\ddot{\phi} + \beta(\phi)\dot{\phi}^2 + \gamma(\phi) = 0 \quad (12)$$

along the virtual manifold (6) and the closed-loop zero dynamics are governed by the scalar homogeneous equation (12), which possesses a  $T$ -periodic solution  $\phi^\Gamma(t)$  due to a specific choice of the virtual constraint (6) and which comes with

$$\alpha(\phi^\Gamma(t)) \neq 0 \text{ for all } t. \quad (13)$$

In turn, dynamics (9) pre-determine the reference torque values  $\tau^*(t)|_{\zeta=\dot{\zeta}=0} = \tau^\Gamma(t)$  along the virtual constraint (6) such that the relation

$$R(0, 0, \phi^\Gamma, \dot{\phi}^\Gamma) + N(0, \phi^\Gamma)\tau^\Gamma = 0 \quad (14)$$

holds true. Provided that  $N(0, \phi^\Gamma, \dot{\phi}^\Gamma)$  is invertible, it follows that

$$\tau^\Gamma(t) = -N^{-1}(0, \phi^\Gamma(t))R(0, 0, \phi^\Gamma(t), \dot{\phi}^\Gamma(t)) \quad (15)$$

is a  $T$ -periodic function along with  $\phi^\Gamma(t)$ .

Once the reference dynamics (3) are rewritten in the new coordinates (8), their partial feedback linearization

$$\ddot{\zeta} = \omega \quad (16)$$

is achieved with the reference state transformation

$$\omega = R(\zeta, \dot{\zeta}, \phi, \dot{\phi}) + N(\zeta, \phi)\tau^*, \quad (17)$$

determined by the right-hand side of (9) and therefore nullified  $\omega(t)|_{\zeta=\dot{\zeta}=0} = \omega^\Gamma(t) = 0$  on the virtual manifold (6). As a matter of fact, relation (17) introduces additional transversal coordinates, corresponding to actuator (nonmechanical) dynamics. Provided that the matrix  $N(\zeta, \phi)$  in (9) is invertible, the above transformation is invertible as well and

$$\tau^*(\zeta, \dot{\zeta}, \phi, \dot{\phi}, \omega) = N^{-1}(\zeta, \phi)[\omega - R(\zeta, \dot{\zeta}, \phi, \dot{\phi})]. \quad (18)$$

To complete the partial transversal linearization (16) the integral function

$$\mathcal{I}(\phi, \dot{\phi}, \phi_0, \phi_1) = \dot{\phi}^2 - \Psi(\phi, \phi_0) \left[ \phi_1^2 - \int_{\phi_0}^{\phi} \Psi(\phi_0, s) \frac{2\gamma(s)}{\alpha(s)} ds \right], \quad (19)$$

specified with

$$\Psi(\phi, \phi_0) = \exp \left\{ - \int_{\phi_0}^{\phi} \frac{2\beta(s)}{\alpha(s)} ds \right\}, \quad (20)$$

is additionally involved to quantify a measure of the distance of the state trajectory from the orbit

$$\phi^\Gamma(t), \zeta_1^\Gamma(t) = 0, \dots, \zeta_{n-1}^\Gamma(t) = 0, \omega^\Gamma(t) = 0 \quad (21)$$

generated by the periodic solution  $\phi^\Gamma(t)$  of (12). It is well-known Shiriaev *et al.* (2006) that the function  $\mathcal{I}(\phi(t), \dot{\phi}(t), \phi_0, \phi_1)$ , thus specified, preserves the zero value along the solutions of equation (12), initialized with  $\phi(0) = \phi_0, \dot{\phi}(0) = \phi_1$ . Moreover, viewed along solutions of (10),  $\mathcal{I}(\phi(t), \dot{\phi}(t), \phi_0, \dot{\phi}_0)$  is governed by

$$\frac{d}{dt}\mathcal{I} = \frac{2\dot{\phi}}{\alpha(\phi)} \left[ \tilde{\mu}(\zeta, \dot{\zeta}, \phi, \dot{\phi}, \omega) - \beta(\phi)\mathcal{I} \right] \quad (22)$$

where

$$\tilde{\mu}(\zeta, \dot{\zeta}, \phi, \dot{\phi}, \omega) = \mu(\zeta, \dot{\zeta}, \phi, \dot{\phi}, \tau^*(\zeta, \dot{\zeta}, \phi, \dot{\phi}, \omega)), \quad (23)$$

and  $\mu$  and  $\tau^*$  are given by (11) and (18), respectively.

Along with  $\zeta$  and  $\dot{\zeta}$ , the above variable  $\mathcal{I}(\phi(t), \dot{\phi}(t), \phi_0, \phi_1)$  composes the coordinate basis, which is transversal to the virtual constraint (6). In order to arrive at the transversal dynamics linearization

it remains to complete the partially feedback linearized dynamics (16) of the reference model (3) with the linearization

$$\delta\dot{\mathcal{I}} = \frac{2\dot{\phi}^\Gamma}{\alpha(\phi^\Gamma)} \left[ \mu_1^\Gamma(t)\delta\zeta + \mu_2^\Gamma(t)\delta\dot{\zeta} + \mu_3^\Gamma(t)\delta\omega - \beta(\phi^\Gamma)\delta\mathcal{I} \right] \quad (24)$$

of (22) around orbit (21) where the transversal variations  $\delta\zeta, \delta\dot{\zeta}, \delta\omega$  are subject to  $\delta\ddot{\zeta} = \delta\omega$ . Hereinafter, the notation

$$\mu_i^\Gamma(t) = \mu_i(0, 0, \phi^\Gamma, \dot{\phi}^\Gamma), \quad i = 1, 2, 3 \quad (25)$$

stand for the  $T$ -periodic functions (11), evaluated along the chosen orbit (21).

Up to now, nothing else than the standard VC approach of Shiriaev *et al.* (2005) was applied to derive the transversal linearization (16), (24) of the reference dynamics (3). A nontrivial extension of the VC approach is subsequently required to linearize the reference input dynamics (4) in the transversal coordinates. Such an extension is developed next.

Differentiating the transformed state (17) and taking into account the reference input equation (4) yield

$$\dot{\omega} = \dot{R} + (\dot{N} - NA_\tau)\tau^* + NB_\tau\nu^* \quad (26)$$

where for ease of reference,  $\dot{N}$  stands for  $dN(\zeta(t), \phi(t))/dt$  and  $\dot{R}$  for  $dR(\zeta(t), \dot{\zeta}(t), \phi(t), \dot{\phi}(t))/dt$ . To linearize (26) it suffices to substitute the input transformation

$$V = \dot{R} + (\dot{N} - NA_\tau)\tau^* + NB_\tau\nu^* \quad (27)$$

into the right-hand side of (26). The equation

$$\dot{\omega} = V \quad (28)$$

thus obtained is coupled to (16), (24), to derive the augmented transversal linearization

$$\delta\dot{\eta} = A_\eta(t)\delta\eta + B_\eta\delta V, \quad (29)$$

specified with

$$\delta\eta = \left[ \delta\mathcal{I} \quad \delta\zeta \quad \delta\dot{\zeta} \quad \delta\omega \right]^T \quad (30)$$

$$A_\eta(t) = \begin{bmatrix} -\frac{2\dot{\phi}^\Gamma}{\alpha(\phi^\Gamma)}\beta(\phi^\Gamma) & \frac{2\dot{\phi}^\Gamma}{\alpha(\phi^\Gamma)}\mu_1^\Gamma & \frac{2\dot{\phi}^\Gamma}{\alpha(\phi^\Gamma)}\mu_2^\Gamma & \frac{2\dot{\phi}^\Gamma}{\alpha(\phi^\Gamma)}\mu_3^\Gamma \\ 0 & 0 & I & 0 \\ 0 & 0 & 0 & I \\ 0 & 0 & 0 & 0 \end{bmatrix} \quad (31)$$

$$B_\eta = \left[ 0 \quad 0 \quad 0 \quad I \right]^T \quad (32)$$

of the over-all reference model (3), (4). Hereinafter,  $I$  stands for the identity matrix of an appropriate dimension.

To complete the reference model design it remains to determine a virtual input  $V$ , exponentially stabilizing the linearized system (29) around the pre-specified orbit (21). Provided that the linear periodic system (29) is completely controllable over the period  $T$ , this can be done (see, e.g., Rugh

(1996); Yakubovich (1986)), for instance, by minimizing the performance index

$$J(\delta\eta, \delta V) = \frac{1}{2} \int_0^\infty [\delta\eta^T D \delta\eta + \delta V^T \delta V] dt \quad (33)$$

along the trajectories of (29) with some positive definite matrix  $D$ . The resulting linear quadratic regulator (LQR)

$$\delta V = -B_\eta^T \delta P(t) \delta\eta \quad (34)$$

is then obtained (see, e.g., Anderson & Moore (1989), Colaneri (2000)) with a positive definite  $T$ -periodic solution  $\delta P(t)$  of the corresponding periodic differential Riccati equation

$$-\delta \dot{P} = \delta P(t) A_\eta(t) + A_\eta^T \delta P(t) + D^T D - \delta P(t) B_\eta B_\eta^T \delta P(t). \quad (35)$$

Based on the time-varying feedback (35), exponentially stabilizing the transversal linearization of the reference model, the following time-invariant input

$$\nu^* = -(NB_\tau)^{-1} [B_\eta \delta P(t(q^*, \dot{q}^*, \tau^*)) \eta + \dot{R} + (\dot{N} - NA_\tau) \tau^*] \quad (36)$$

is extracted from (27) with  $\eta = (\mathcal{I}, \zeta, \dot{\zeta}, \omega)^T$  and with  $V = -B_\eta^T \delta P(t(q^*, \dot{q}^*, \tau^*)) \eta$ , which is inherited from (34) with the projection operator  $t(q^*, \dot{q}^*, \tau^*)$ , substituted for  $t$ . The projection operator  $t(q^*, \dot{q}^*, \tau^*)$  is constructed as in Shiriaev *et al.* (2010); Pchelkin *et al.* (2017) and it is such that at an arbitrary time instant  $t$ , the generalized coordinates  $q^*(t), \dot{q}^*(t), \tau^*(t)$  belong to the Poincare section, moving along the desired orbit (21). As a matter of fact, all the variables in the right-hand side of (36) should be expressed in the original coordinates  $q^*, \dot{q}^*, \tau^*$  by means of relations (7), (17), (19).

Under certain conditions, the autonomous feedback (36) steers the reference model dynamics (3), (4) to the chosen orbit (21). The following result is thus obtained.

**Proposition 1:** *Consider the reference model (3), (4) with the assumptions above. Suppose that*

1. *there is a virtual constraint (6) such that the corresponding zero reference dynamics equation (12) satisfies (13) and possesses a nontrivial  $T$ -periodic solution  $\phi^\Gamma$ ;*
2. *the matrix  $N(\zeta, \phi)$  in (9) is locally nonsingular around orbit (21), generated by the periodic solution  $\phi^\Gamma$  of (12);*
3. *the linear periodic system (29) is completely controllable over the period  $T$ .*

*Then the closed-loop system (3), (4), fed by the reference input (36), which is expressed in the original coordinates  $q^*, \dot{q}^*, \tau^*$  by means of relations (7), (17), (19), is orbitally exponentially stable around the pre-specified orbit (21).*

*Proof* follows the line of reasoning used in that of (Shiriaev *et al.*, 2010, Theorem 3). By construction, made under the conditions of the proposition, the linear periodic system (29), driven by (34), represents the transversal linearization of the closed-loop system (3), (4), (36) around the pre-specified orbit (21). Since this linearization (29), (34) is exponentially stable due to the LQR design the Andronov-Vitt theorem Andronov & Vitt (1933) (see also Leonov (2006); Pchelkin *et al.* (2017)) becomes applicable to the closed loop system in question, the monodromy matrix of which possesses all eigenvalues within the unit circle but the one of the unit value. The exponential orbital stability of the closed-loop system is then established by applying the Andronov-Vitt theorem. Proposition 1 is thus proved.

Later on, numerical evidences, supporting Proposition 1, will be presented for a cart-pendulum testbed.

## 2.2 Nonlinear $\mathcal{H}_\infty$ output feedback generation of periodic motion

At the second step, the constructed system (3), (4), (36) is viewed as a reference model to be tracked. Since by construction, the trajectories of the reference model (3), (4), (36) are bounded and exponentially converging to a periodic solution along the designed reference orbit, the robust periodic motion generation of the plant dynamics (1), (2) can then be achieved by means of the nonlinear output feedback synthesis from Orlov & Aguilar (2014), applied to the error dynamics written in terms of the state-input error

$$e^T = [e_p^T, \dot{e}_p^T, e_a^T] = [(q - q^*)^T, (\dot{q} - \dot{q}^*)^T, (\tau - \tau^*)^T] \text{ and } u = (\nu - \nu^*)^T \quad (37)$$

with respect to that of the reference model. Clearly, these dynamics are governed by

$$\dot{e} = f(e, t) + g_1(e, t)w + g_2u \quad (38)$$

where

$$f(e, t) = \begin{bmatrix} M^{-1}(e_p + q^*)[-C(e_p + q^*, \dot{e}_p + \dot{q}^*)(\dot{e}_p + \dot{q}^*) - G(e_p + q^*)] \\ -A_\tau e_a \end{bmatrix} +$$

$$\begin{bmatrix} 0 \\ M^{-1}(e_p + q^*)[M(q^*)\ddot{q}^* + C(q^*, \dot{q}^*)\dot{q}^* + G(q^*)] - \ddot{q}^* + M^{-1}(e_p + q^*)Be_a \\ 0 \end{bmatrix}$$

$$g_1(e, t) = \begin{bmatrix} 0_{n \times n} & 0_{n \times k} & 0_{n \times l} \\ M^{-1}(e_p + q^*) & 0_{n \times k} & 0_{n \times l} \\ 0_{k \times n} & I_{k \times k} & 0_{k \times l} \end{bmatrix}$$

$$g_2 = \begin{bmatrix} 0_{n \times k} \\ 0_{n \times k} \\ B_\tau \end{bmatrix}$$

$$w = (w_q^T, w_\tau^T, w_y^T)^T. \quad (39)$$

Along with the plant disturbances  $w_q \in \mathbb{R}^n$  and actuator disturbances  $w_\tau \in \mathbb{R}^{n-1}$ , the augmented disturbance vector  $w \in \mathbb{R}^{2n+l-1}$  has additionally been composed of the measurement noise  $w_y \in \mathbb{R}^l$  to be introduced into state measurements, available for the output feedback.

It is straightforward to verify that  $f(0, t) = 0$  for all  $t$  what allows one to formally apply the nonlinear  $\mathcal{H}_\infty$  synthesis to the error system (38), whose disturbance-free dynamics possess an equilibrium in the origin.

In the sequel, the error output  $z \in \mathbb{R}^s$  to be controlled as well as the measurement vector  $y \in \mathbb{R}^p$ , available for feedback, are given in the generic forms

$$z(t) = h_1(e(t), t) + k_{12}(e(t), t)u \quad (40)$$

and

$$y(t) = h_2(e(t), t) + k_{21}(e(t), t)w \quad (41)$$

with some matrix/vector functions  $h_1, h_2, k_{12}, k_{21}$  of appropriate dimensions subject to the well-known simplifying assumptions

$$h_1^T(e, t)k_{12}(e, t) \equiv 0, \quad k_{12}^T(e, t)k_{12}(e, t) \equiv I \quad (42)$$

$$k_{21}(e, t)g_1^T(e, t) \equiv 0, \quad k_{21}(e, t)k_{21}^T(e, t) \equiv I, \quad (43)$$

typically used in the nonlinear  $\mathcal{H}_\infty$  output feedback design Isidori & Astolfi (1992).

The problem of the nonlinear  $\mathcal{H}_\infty$  output feedback design to be solved at the second step is in finding an output feedback controller  $\mathcal{K}(y)$  (if any), asymptotically stabilizing the disturbance-free ( $w \equiv 0$ ) error dynamics (37), (38) such that the  $\mathcal{L}_2$ -gain of the disturbed system (37)-(41) is less than a certain  $\gamma > 0$ , that is the inequality

$$\int_{t_0}^T \|z(t)\|^2 dt \leq \gamma^2 \int_{t_0}^T \|w(t)\|^2 dt \quad (44)$$

holds for all  $T > t_0$  and all piecewise-continuous disturbances  $w(t)$  for which the state trajectory of the closed-loop system, starting from the initial point  $e(t_0) = 0$  remains in some neighborhood  $\mathcal{U}$  of the origin for all  $t \in [t_0, T]$ . Since by the feasibility of the reference model, the error dynamics (38) are locally controllable around the origin, such a problem is guaranteed Isidori & Astolfi (1992) to possess a solution provided that the error system (38) is locally observable over the measurement output (41).

The stabilizing output feedback law

$$u = -g_2^T P_\epsilon \xi, \quad (45)$$

solving the problem in question, is inherited from Orlov & Aguilar (2014) and it is fed by the state estimator

$$\dot{\xi} = f(\xi, t) + \left[ \frac{1}{\gamma^2} g_1(\xi, t) g_1^T(\xi, t) - g_2(\xi, t) g_2^T(\xi, t) \right] P_\epsilon(t) \xi + Z_\epsilon(t) C_2^T(t) [y - h_2(\xi, t)], \quad (46)$$

constructed over the measured output (41), where the nonlinear functions  $f, g_1, g_2$  are associated with the error plant representation (37)-(63), and  $P_\epsilon$  and  $Z_\epsilon$  are positive definite periodic solutions of the differential Riccati equations

$$\begin{aligned} -\dot{P}_\epsilon &= P_\epsilon(t)A(t) + A^T(t)P_\epsilon(t) + C_1^T(t)C_1(t) \\ &+ P_\epsilon(t) \left[ \frac{1}{\gamma^2} B_1 B_1^T - B_2 B_2^T \right] (t) P_\epsilon(t) + \epsilon I, \end{aligned} \quad (47)$$

$$\begin{aligned} \dot{Z}_\epsilon &= \tilde{A}(t)Z_\epsilon(t) + Z_\epsilon \tilde{A}^T(t) + B_1(t)B_1^T(t) \\ &+ Z_\epsilon(t) \left[ \frac{1}{\gamma^2} P_\epsilon(t)B_2(t)B_2^T(t)P_\epsilon(t) - C_2^T(t)C_2(t) \right] Z_\epsilon(t) + \epsilon I \end{aligned} \quad (48)$$

specified with

$$A(t) = \frac{\partial f}{\partial e}(0, t), \quad B_1(t) = g_1(0, t), \quad B_2 = g_2, \quad \tilde{A}(t) = A(t) + \gamma^{-2} B_1(t)B_1^T(t)P_\epsilon(t), \quad (49)$$

and some positive  $\epsilon$ .

The proposed synthesis is summarized as follows.

**Proposition 2:** *Consider the error dynamics (38), governing the deviation vector (37) of the plant state (1), (2) from that of the reference model (3), (4), (36). Suppose that there exist positive definite  $T$ -periodic solutions of the differential Riccati equations<sup>1</sup> (47), (48) and let the error dynamics (38) be driven by the dynamic output feedback (45), (46). Then the disturbance-free closed-loop system (38), (45), (46) is asymptotically stable and its disturbed version locally possesses the  $\mathcal{L}_2$ -gain less than  $\gamma > 0$ .*

*Proof.* Since the plant and actuator dynamics are governed by smooth ordinary differential equations, the above proposition is nothing else than the assertion of (Orlov & Aguilar, 2014, Theorem 25, p. 94), specified to a particular case of the generic system, given in the form of the error system (37)-(49).

In what follows, capabilities of the proposed synthesis procedure and its robustness features are illustrated in a case study of the underactuation degree one. To facilitate the exposition, this study is confined to a practical situation where only noise-corrupted position measurements of the plant are available for the feedback design while the plant velocities and the actuated torques remain unavailable. Potential extensions to mechanical systems of higher underactuation degrees prove to be possible whenever the VC approach remains feasible. Being of practical interest, such extensions are however beyond the present investigation.

### 3. Case Study: Model Reference Orbital Stabilization of Voltage-driven Cart-pendulum Model

A cart-pendulum model of interest is depicted in Fig. 1 and it is governed by (1), (2), specified with

$$\begin{aligned} n = 2, \quad k = 1, \quad q = (q_1, q_2)^T, \quad \dot{q} = (\dot{q}_1, \dot{q}_2)^T, \quad A_\tau = a, \quad B_\tau = b, \\ M(q) = \begin{bmatrix} 2 & \cos q_2 \\ \cos q_2 & 1 \end{bmatrix}, \quad C(q, \dot{q}) = \begin{bmatrix} 0 & -\dot{q}_2 \sin q_2 \\ 0 & 0 \end{bmatrix}, \\ G(q) = \begin{bmatrix} 0 \\ -g \sin q_2 \end{bmatrix}, \quad B = \begin{bmatrix} 1 \\ 0 \end{bmatrix} \end{aligned} \quad (50)$$

where  $q_1$  is the horizontal displacement of the cart,  $q_2$  is the angle between the vertical and the rod of the pendulum, which is zero in the upper position,  $\tau$  is the torque force, generated by the electrical motor and acting in the horizontal direction,  $\nu$  is the voltage applied to the electrical motor and  $g$  is the gravitation constant. In contrast to Shiriaev *et al.* (2005), the above cart-pendulum model is driven by the voltage  $\nu$ , rather than directly by the torque force  $\tau$ .

---

<sup>1</sup>The existence of such solutions is well-known Orlov & Aguilar (2014) to ensure the local controllability and observability of the error system in question.

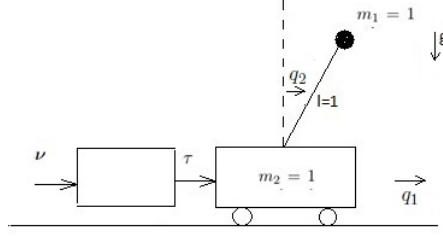


Figure 1.: Cart-pendulum model

In the numerical verification of the proposed synthesis procedure, subsequently made for the above car-pendulum testbed, the output (40) is specified with

$$h_1(e, t) = C_1 e, \quad C_1 = \begin{bmatrix} 0 & 0 & 0 & 0 & 0 \\ 10 & 0 & 0 & 0 & 0 \\ 0 & 0.001 & 0 & 0 & 0 \\ 0 & 0 & 0.001 & 0 & 0 \\ 0 & 0 & 0 & 0.001 & 0 \\ 0 & 0 & 0 & 0 & 0.15 \end{bmatrix}, \quad k_{12}(e, t) = [1 \ 0 \ 0 \ 0 \ 0 \ 0]^T \quad (51)$$

where the numerical parameters are chosen by trials and errors to get an appropriate performance of the closed-loop and the state deviation vector in (37) is simplified to

$$e^T = [e_p^T, \dot{e}_p^T, e_a^T] = [(q_1 - q_1^*)^T, (q_2 - q_2^*)^T, (\dot{q}_1 - \dot{q}_1^*)^T, (\dot{q}_2 - \dot{q}_2^*)^T, (\tau - \tau^*)^T]. \quad (52)$$

For certainty, the available measurement (41) is confined to

$$h_2(e, t) = \underbrace{[I_{2 \times 2} \ 0_{2 \times 3}]}_{C_2} e, \quad k_{21}(e, t) = [0_{2 \times 3} \ I_{2 \times 2}], \quad (53)$$

thus ruling out the plant velocities  $\dot{q}_1, \dot{q}_2$  and the actuator state  $\tau$  from the feedback design.

### 3.1 Cart-pendulum reference model

In order to make the generic reference model (3), (4) to match that of the cart-pendulum it is specified with (50). Such a cart-pendulum reference model is well-known Shiriaev *et al.* (2005) to be capable of generating an orbit around the upright position of the pendulum provided that it is driven along the virtual constraint

$$q_1^*(t) + L \sin q_2^*(t) - d = 0 \quad (54)$$

with design parameters  $L > 1$  and  $d$ . It is worth of noticing that the above constraint (54) has been recognized to preserve a particular point of the pendulum, separated by distance  $L$  from the suspension point, on the vertical line  $q_1^* = d$ . Condition 1 of Proposition 1 is thus satisfied for the cart-pendulum dynamics (3), (4), (50), confined to the virtual constraint (54).

The general virtual constraint (6) of the afore-given cart-pendulum model (3), (4), (50) is thus

effectively chosen with

$$\phi = q_2^* \text{ and } r_1(\phi) = d - L \sin \phi. \quad (55)$$

In the new coordinates

$$\phi = q_2^*, \quad \zeta = d - L \sin \phi, \quad (56)$$

corresponding to (8), the reference dynamics (9) and (10) are further specified with  $\alpha(\phi) = 1 - L \cos^2 \phi$ ,  $\beta(\phi) = L \cos \phi \sin \phi$ ,  $\gamma(\phi) = -g \sin \phi$ ,

$$N(\zeta, \phi) = \frac{L \cos^2 \phi - 1}{\cos^2 \phi - 2}, \quad (57)$$

$$R(\zeta, \dot{\zeta}, \phi, \dot{\phi}) = \frac{\sin \phi (-\dot{\phi}^2 + g \cos \phi) + L \cos \phi (-2g \sin \phi + \dot{\phi}^2 \sin \phi \cos \phi)}{\cos^2 \phi - 2} - L \dot{\phi}^2 \sin \phi \quad (58)$$

and

$$\mu(\zeta, \dot{\zeta}, \phi, \dot{\phi}^*, \tau^*) = -\cos(\phi)\omega \quad (59)$$

that can straightforwardly be verified by double differentiating (55). It is clear that under  $L > 1$ , relation (57), determining the matrix  $N(\zeta, \phi)$ , proves to be invertible, thereby ensuring Condition 2 of Proposition 1.

The transversal linearization (16) and (24) is then specified with  $\mu_1^\Gamma(t) = \mu_2^\Gamma(t) = 0$  and  $\mu_3^\Gamma(t) = -\cos(\phi^\Gamma)$  where

$$\phi^\Gamma(t) = \phi^\Gamma(t + T) \quad (60)$$

is a periodic solution of (12). Coupled to the corresponding feedback linearization (28) of the torque dynamics, the transversal linearization (16), (24) results in the augmented plant-actuator linearization (29) of the cart-pendulum reference model, which is specified with

$$A_\eta = \begin{bmatrix} -\frac{2L\dot{\phi}^\Gamma \cos \phi^\Gamma \sin \phi^\Gamma}{(1-L \cos^2 \phi^\Gamma)} & 0 & 0 & -\frac{2\dot{\phi}^\Gamma \cos \phi^\Gamma}{(1-L \cos^2 \phi^\Gamma)} \\ 0 & 0 & 1 & 0 \\ 0 & 0 & 0 & 1 \\ 0 & 0 & 0 & 0 \end{bmatrix}, \quad B_\eta = \begin{bmatrix} 0 \\ 0 \\ 0 \\ 1 \end{bmatrix} \quad (61)$$

and which is completely controllable over the period  $T$  because its reduced-order torque-driven model

$$\dot{\mathcal{I}} = -\frac{2L\dot{\phi}^\Gamma \cos \phi^\Gamma \sin \phi^\Gamma}{(1-L \cos^2 \phi^\Gamma)} \mathcal{I} - \frac{2\dot{\phi}^\Gamma \cos \phi^\Gamma}{(1-L \cos^2 \phi^\Gamma)} \omega, \quad \ddot{\zeta} = \omega \quad (62)$$

has been verified in Shiriaev *et al.* (2005) to be so. Hence, Condition 3 of Proposition 1 holds true as well.

The reference input, constructed according to (34) and expressed in the original coordinates  $q_1^*$ ,  $\dot{q}_1^*$ ,  $q_2^*$ ,  $\dot{q}_2^*$ ,  $\tau^*$  by means of the corresponding relations (7), (17), finalizes the reference model design which, by applying Proposition 1, turns out to be appropriate for the periodic motion generation of the voltage-driven cart-pendulum testbed. Summarizing, the following result is in order.

**Proposition 3:** *Consider the cart-pendulum reference model (3), (4), specified with (50). Let the virtual constraint (54) be invoked to design the corresponding reference input (36) in the transverse coordinates and let this input be further expressed in the original coordinates  $q_1^*$ ,  $\dot{q}_1^*$ ,  $q_2^*$ ,  $\dot{q}_2^*$ ,  $\tau^*$  by means of the corresponding relations (7), (18) to feed the cart-pendulum model. Then the closed-loop reference system, thus constructed, is orbitally exponentially stable around the pre-specified orbit (21), generated by the periodic motion (60) along the virtual constraint (54).*

*Proof.* Since the conditions of Proposition 1 have earlier been validated for the underlying cart-pendulum reference model the proof is completed by applying Proposition 1 to the model in question.

### 3.2 Robust orbitally stabilizing position feedback synthesis

In order to apply the periodic motion synthesis, established in Section 2, the error cart-pendulum dynamics should first be embedded into the generic form (37)-(44), using the relevant specifications (50)-(53). The desired model reference tracking of the cart-pendulum model is then achieved with the properly specified synthesis procedure of Proposition 2.

**Proposition 4:** *Let the deviation vector (52) be determined in terms of the cart-pendulum state (1), (2), (50) and that of the reference model (3), (4), (36) of Proposition 3. Suppose that there exist positive definite  $T$ -periodic solutions of the differential Riccati equations (47), (48), matching to the error dynamics (38) of the evolution of the deviation vector specified above. Then the disturbance-free closed-loop system (38), driven by the corresponding dynamic position feedback (45), (46), is asymptotically stable and its disturbed version locally possesses the  $\mathcal{L}_2$ -gain less than  $\gamma > 0$ .*

*Proof* is confined to the straightforward application of Proposition 2 to the particular system in question.

Performance issues of the proposed model reference tracking of the voltage-driven cart-pendulum are numerically illustrated in the next subsection.

### 3.3 Simulation results

The periodic motion generation along the virtual constraint (54) was numerically tested for the cart-pendulum model (1), (2), (50), driven by the voltage (45), (46), applied to the electrical motor. Simulations were performed with Simulink for the model values shown in Table 1.

Table 1.: Model values of the voltage-driven cart-pendulum prototype and of its reference model.

Parameter	Symbol	Value
Virtual constraint	$L$	1.5
Virtual constraint	$d$	0
Actuator	$a$	5
Actuator	$b$	5
Initial conditions for the reference model	$[q_1^*(0) \ \dot{q}_1^*(0) \ q_2^*(0) \ \dot{q}_2^*(0) \ \tau^*(0)]^T$	$[0 \ -0.15 \ 0.1 \ 0 \ 0.1]^T$
Initial conditions for the plant	$[q_1(0) \ \dot{q}_1(0) \ q_2(0) \ \dot{q}_2(0) \ \tau(0)]^T$	$[0.1 \ -0.1 \ 0.4 \ -0.2 \ 0.3]^T$
$\mathcal{H}_\infty$ Differential Riccati equations	$\epsilon$	0.1
$\mathcal{H}_\infty$ Differential Riccati equations	$\gamma$	400
LQR Differential Riccati equation	$D$	$I_{4 \times 4}$
Cart-pendulum perturbations	$w_q = [w_x \ w_\theta]^T$	$[0 \ 0]^T / [0.1\sin(t) \ 0.1\sin(t)]^T$
Actuator perturbation	$w_\tau$	$0 / 0.1 \sin(t)$
Measurements perturbations	$w_y = [w_{y1} \ w_{y2}]^T$	$[0 \ 0]^T / [0.05\sin(2t) \ 0.05\sin(2t)]^T$

Table 2.: Model values of the torque-driven cart-pendulum prototype and of its reference model.

Parameter	Symbol	Value
Virtual constraint	$L$	1.5
Virtual constraint	$d$	0
Initial conditions for the reference model	$[q_1^*(0) \quad \dot{q}_1^*(0) \quad q_2^*(0) \quad \dot{q}_2^*(0)]^T$	$[0 \quad -0.15 \quad 0.1 \quad 0]^T$
Initial conditions for the plant	$[q_1(0) \quad \dot{q}_1(0) \quad q_2(0) \quad \dot{q}_2(0)]^T$	$[0.1 \quad -0.1 \quad 0.4 \quad -0.2]^T$
$\mathcal{H}_\infty$ Differential Riccati equations	$\epsilon$	0.1
$\mathcal{H}_\infty$ Differential Riccati equations	$\gamma$	400
LQR Differential Riccati equation	$D$	$I_{3 \times 3}$
Cart-pendulum perturbations	$w_q = [w_x \quad w_\theta]^T$	$[0 \quad 0]^T / [0.1\sin(t) \quad 0.1\sin(t)]^T$
Measurements perturbations	$w_y = [w_{y1} \quad w_{y2}]^T$	$[0 \quad 0]^T / [0.05\sin(2t) \quad 0.05\sin(2t)]^T$

Following the developed procedure of the periodic motion generation, the orbitally stabilizing synthesis was performed in two steps. At the first step, the reference input (36) was constructed for the cart-pendulum reference model (3), (4) by numerically solving the corresponding Riccati equation (35). At the second step, the output feedback (45), (46) was synthesized by determining numerically appropriate (positive definite periodic) solutions of the corresponding Riccati equations (47), (48), which arise in the nonlinear  $\mathcal{H}_\infty$  design. By iteration, a feasible attenuation level  $\gamma = 400$  and reasonably small  $\epsilon = 0.1$  were detected in order to obtain the required solutions  $P_\epsilon$ ,  $Z_\epsilon$  of (47), (48). The interested reader may refer to Orlov & Aguilar (2014) for relevant technical details on such an iteration procedure of solving Riccati differential equations.

For comparison, the periodic motion generation was additionally tested for the torque-driven cart-pendulum model. As shown in Table 2, the same parameter values and initial conditions were used in the simulation runs for both voltage- and torque-driven cart-pendulum models in order to make a fair comparison. On one hand, the voltage actuation has already been synthesized for the cart-pendulum model. On the other hand, the torque actuation is summarized for the cart-pendulum as follows.

Given the cart-pendulum model (1), (50), and its reference model (3), constructed as in Shiriaev *et al.* (2005), the error dynamics (38) in terms of  $e^T = [e_p^T, \dot{e}_p^T] = [(q - q^*)^T, (\dot{q} - \dot{q}^*)^T]$  and  $u = (\tau - \tau^*)^T$  are specified with

$$f(e, t) = \begin{bmatrix} M^{-1}(e_p + q^*)[-C(e_p + q^*, \dot{e}_p + \dot{q}^*)(\dot{e}_p + \dot{q}^*) - G(e_p + q^*) + B\tau^*] - \ddot{q}^* \end{bmatrix}$$

$$g_1(e, t) = \begin{bmatrix} 0_{n \times n} & 0_{n \times l} \\ M^{-1}(e_p + q^*) & 0_{n \times l} \end{bmatrix}$$

$$g_2 = \begin{bmatrix} 0_{n \times n-1} \\ M^{-1}(e_p + q^*)B \end{bmatrix}$$

$$w = (w_q^T, w_y^T)^T. \quad (63)$$

Respectively, the error performance (i.e., output to be controlled) (40) and the available measure-

ment (41) are given by

$$h_1(e, t) = C_1 e, \quad C_1 = \begin{bmatrix} 0 & 0 & 0 & 0 \\ 10 & 0 & 0 & 0 \\ 0 & 0.001 & 0 & 0 \\ 0 & 0 & 0.001 & 0 \\ 0 & 0 & 0 & 0.001 \end{bmatrix},$$

$$k_{12}(e, t) = [1 \ 0 \ 0 \ 0 \ 0]^T, \quad h_2(e, t) = \underbrace{[I_{2 \times 2} \ 0_{2 \times 2}]}_{C_2} e, \quad k_{21}(e, t) = [0_{2 \times 2} \ I_{2 \times 2}]. \quad (64)$$

Following the  $\mathcal{H}_\infty$  control design procedure of Section 2.2, the controller (45) is thus specified for the torque-driven cart-pendulum error dynamics, thereby yielding  $\tau = u + \tau^*$ , where  $\tau^*$  is the control input for the reference model constructed as in Shiriaev *et al.* (2005). While adopting the torque-driven cart-pendulum model, the actuator dynamics are ignored and viewed as a structural disturbance, i.e., it is applied to the cart-pendulum model as if it were driven by voltage.

### 3.3.1 Performance comparison of the cart-pendulum driven by voltage vs. the cart-pendulum driven by torque

Closed-loop dynamics of the cart-pendulum model are numerically studied side by side for the disturbance-free case and for the perturbed case where external and measurement disturbances were applied. Figures 2-7 reflect the nominal closed-loop behavior with  $w = [w_q^T, w_\tau^T, w_y^T]^T = [w_x, w_\theta, w_\tau, w_{y1}, w_{y2}]^T = [0, 0, 0, 0, 0]^T$ , whereas Figures 8-14 correspond to the applied disturbances  $w = [w_q^T, w_\tau^T, w_y^T]^T = [w_x, w_\theta, w_\tau, w_{y1}, w_{y2}]^T = [0.1 \sin(t), 0.1 \sin(t), 0.1 \sin(t), 0.05 \sin(2t), 0.05 \sin(2t)]^T$ .

Figure 2 compares the tracking errors (deviations of the cart-pendulum states from its reference model states) of the undisturbed cart-pendulum, driven by voltage, and the tracking errors of the undisturbed cart-pendulum, driven by torque. Figure 2a shows the 2-norm of the errors the voltage-driven cart-pendulum whereas Figure 2b shows the 2-norm of the tracking errors of the torque-driven cart-pendulum. It is concluded from the figures that both tracking errors escape to zero reasonably fast approximately after 10 s.

Figure 3 compares the estimated deviations of the tracking errors. Figure 3a shows the 2-norm of the tracking error deviation of the voltage-driven model vs. Figure 3b of that of the torque-driven model. It is seen that in both cases the deviations escape to zero after 10 s as well.

Figure 4 depicts reference trajectories on the phase portrait projections of the pendulum angular variable for the voltage-driven reference model and for the torque-driven reference model. In both cases, the trajectories are initialized in the orbit but the one, produced by voltage, shows a deviation from the orbit due to the actuator dynamics. Remarkably, the proposed reference voltage input enforces the motion to the desired orbit despite the actuator dynamics.

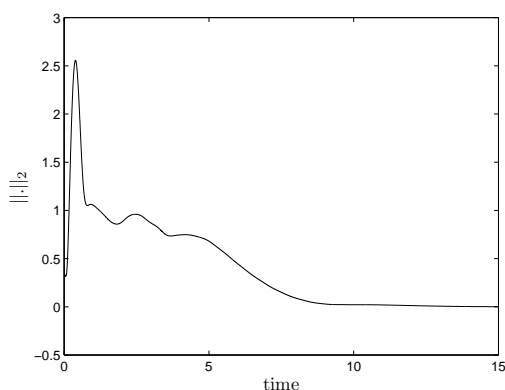
The orbital stabilization of the voltage- and torque-driven pendulums are shown in Figure 5 on the phase portrait projection of the pendulum angular variable. The transitions to the reference orbit are seen to be very similar for both actuators. The resulting (voltage and torque) actuator inputs are presented in Figure 6, both acquire a periodic behavior after about 5 s transitory. As expected, the actuator inputs remain reasonably bounded.

The disturbance-free tracking error and its estimate are shown in Figure 7 for the torque variable, driven by voltage.

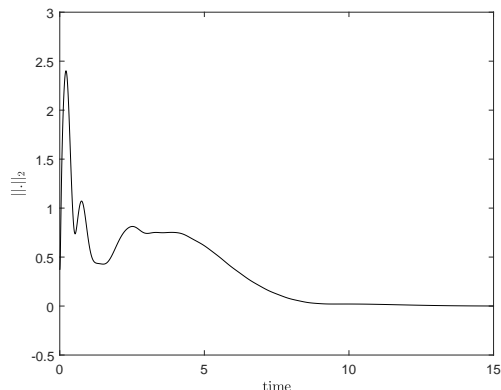
The tracking errors in the presence of disturbances are depicted in Figure 8 for the voltage-driven cart-pendulum vs. the torque-driven cart-pendulum model. Although the disturbances destroy orbital stabilization, however, their influence is attenuated so that the error dynamics remain bounded.

The tracking error estimates under disturbances are shown in Figure 9. Figure 9a shows the 2-norm of the estimate for the voltage control input whereas Figure 9b shows the 2-norm of the estimate for the torque control input. It is seen that in both cases the tracking error estimates remain bounded.

The disturbed angular variables of the voltage-driven cart-pendulum model vs. that of the torque-driven cart-pendulum model are presented in Figure 10 on the phase portrait projection. Although the orbital stabilization around the limit cycle is destroyed by disturbances for either actuator, the resulting angular motions remain bounded, thereby verifying the disturbance attenuation in both cases. The applied voltage and torque inputs, both reasonably bounded, are shown in Figure 11 in the presence of disturbances. Finally, the deviation of the torque from its reference model, computed under disturbances, and the torque estimate are depicted in Figure 12.

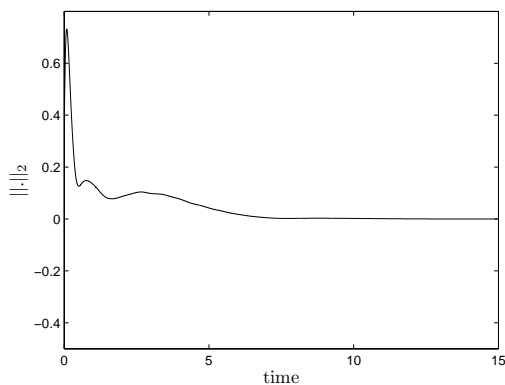


(a) Tracking error  $\|(e_{p_1}, e_{p_2}, \dot{e}_{p_1}, \dot{e}_{p_2})^T\|_2$  for the voltage-driven plant.

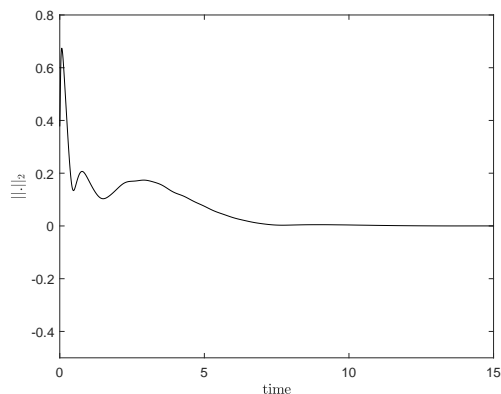


(b) Tracking error  $\|(e_{p_1}, e_{p_2}, \dot{e}_{p_1}, \dot{e}_{p_2})^T\|_2$  for the torque-driven plant.

Figure 2.: Tracking errors between the plant and the reference model in the disturbance-free case.

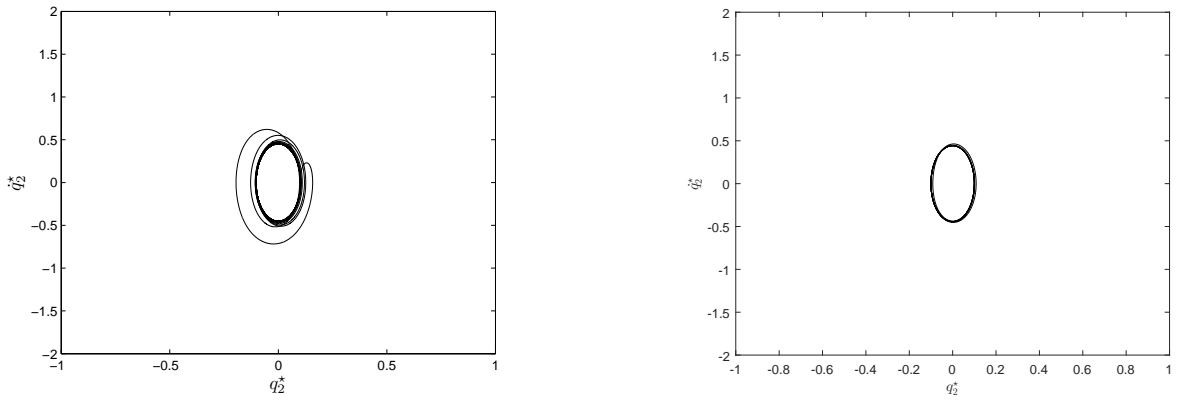


(a) Deviation norm =  $\|(\xi_1 - e_{p_1}, \xi_2 - e_{p_2}, \xi_3 - \dot{e}_{p_1}, \xi_4 - \dot{e}_{p_2})^T\|_2$  for the voltage-driven plant.

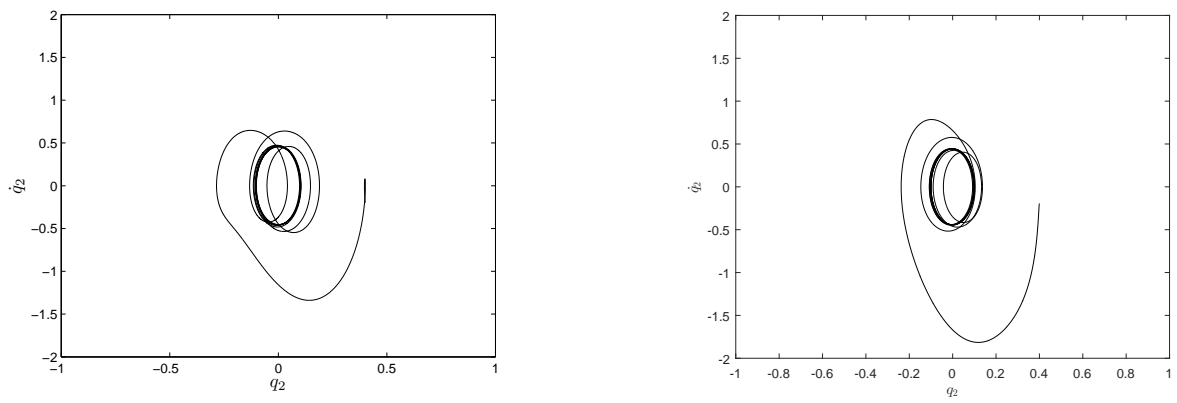


(b) Deviation norm =  $\|(\xi_1 - e_{p_1}, \xi_2 - e_{p_2}, \xi_3 - \dot{e}_{p_1}, \xi_4 - \dot{e}_{p_2})^T\|_2$  for the torque-driven plant.

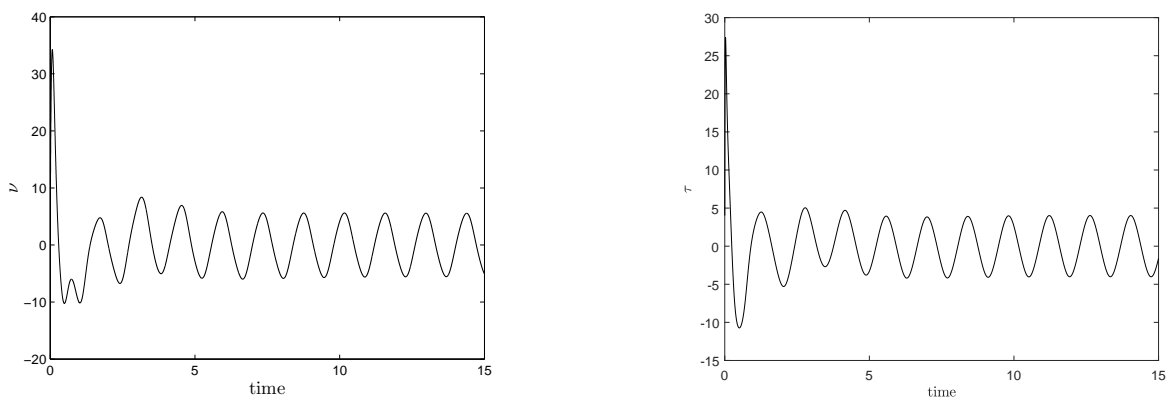
Figure 3.: Deviation of the tracking errors from their estimates in the disturbance-free case.



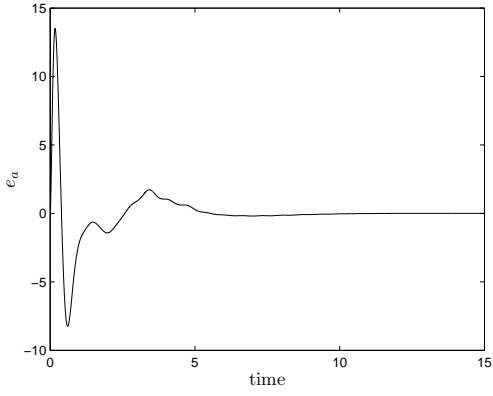
(a) Voltage-driven reference trajectory on  $(q_2^*, \dot{q}_2^*)$ -plane. (b) Torque-driven reference trajectory on  $(q_2^*, \dot{q}_2^*)$ -plane.  
 Figure 4.: Reference trajectories on the phase portrait projections of the pendulum angular variable.



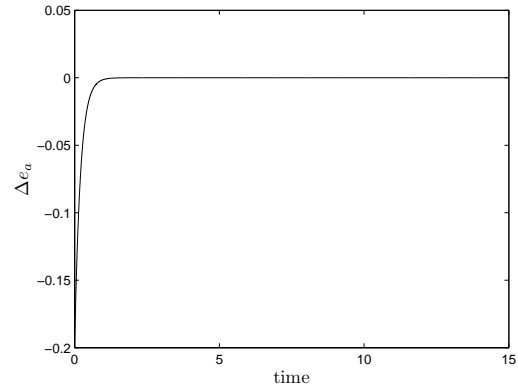
(a) Voltage-driven pendulum motion on  $(q_2, \dot{q}_2)$ -plane. (b) Torque driven pendulum motion  $(q_2, \dot{q}_2)$ -plane.  
 Figure 5.: Disturbance-free orbital stabilization.



(a) Control input for the voltage-driven plant. (b) Control input for the torque-driven plant/  
 Figure 6.: Control inputs  $\nu$  and  $\tau$  in the disturbance-free case.

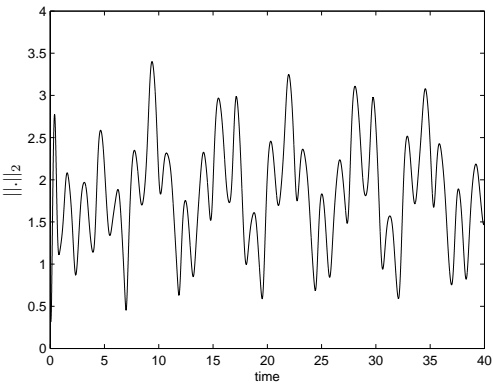


(a) Torque error  $e_a = \tau - \tau^*$ .

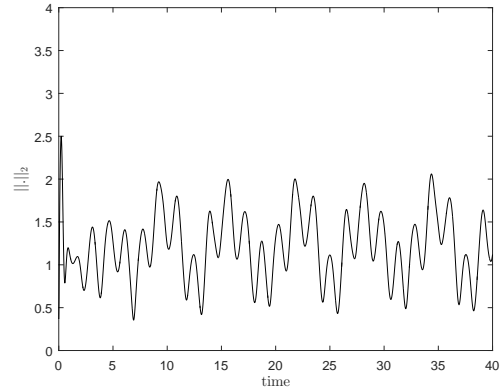


(b) Deviation  $\Delta e_a = \xi_5 - e_a$  of the torque error from its estimate.

Figure 7.: Torque tracking error and its estimate for the disturbance-free voltage-driven plant.

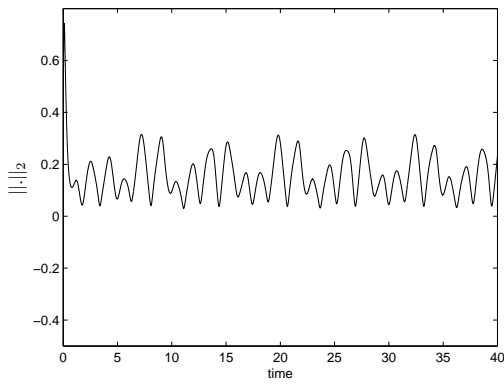


(a) Tracking error  $\|(e_{p1}, e_{p2}, \dot{e}_{p1}, \dot{e}_{p2})^T\|_2$  for the voltage-driven plant.

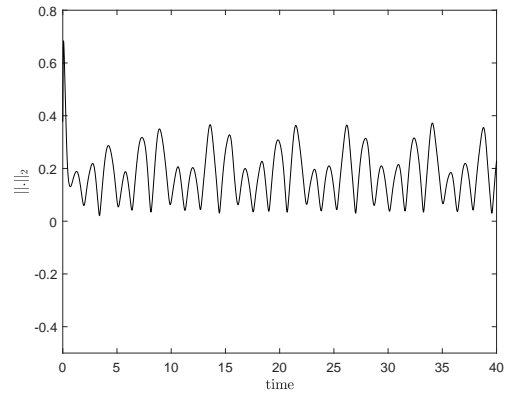


(b) Tracking error  $\|(e_{p1}, e_{p2}, \dot{e}_{p1}, \dot{e}_{p2})^T\|_2$  for the torque-driven plant.

Figure 8.: Tracking errors between the plant and the reference model in the presence of disturbances.

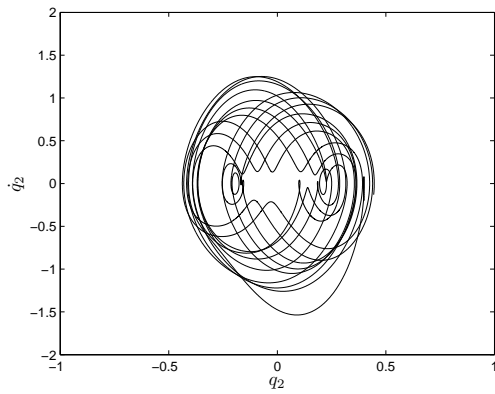


(a) Deviation norm  $= \|(\xi_1 - e_{p1}, \xi_2 - e_{p2}, \xi_3 - \dot{e}_{p1}, \xi_4 - \dot{e}_{p2})^T\|_2$  of the voltage-driven plant.

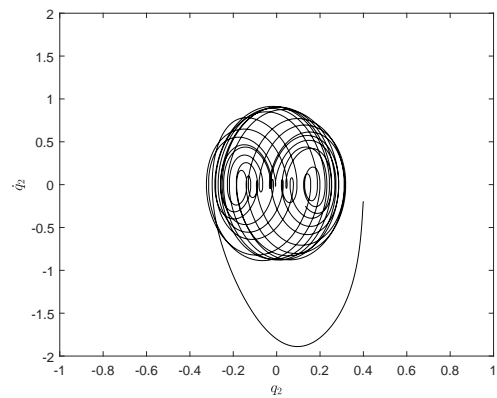


(b) Deviation norm  $= \|(\xi_1 - e_{p1}, \xi_2 - e_{p2}, \xi_3 - \dot{e}_{p1}, \xi_4 - \dot{e}_{p2})^T\|_2$  of the torque-driven plant.

Figure 9.: Deviation of the tracking errors from their estimates in the presence of disturbances.

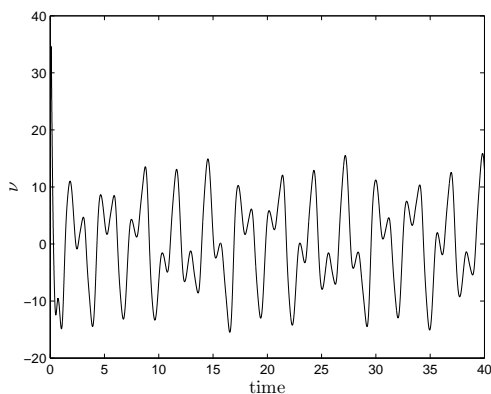


(a) Voltage-driven angular trajectory on  $(q_2, \dot{q}_2)$ -plane.

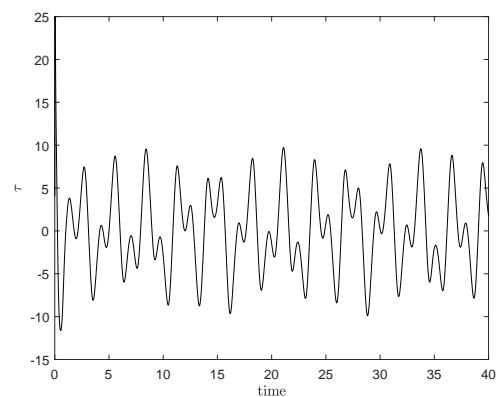


(b) Torque-driven angular trajectory on  $(q_2, \dot{q}_2)$ -plane.

Figure 10.: Disturbance attenuation: pendulum motion on the phase portrait projection.



(a) Control input for the voltage-driven plant.



(b) Control input for the torque-driven plant.

Figure 11.: Control inputs  $\nu$  and  $\tau$  in the presence of disturbances.

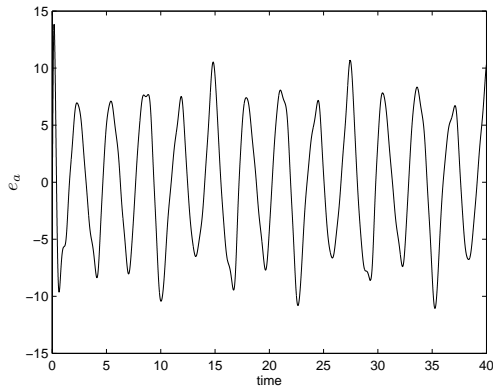
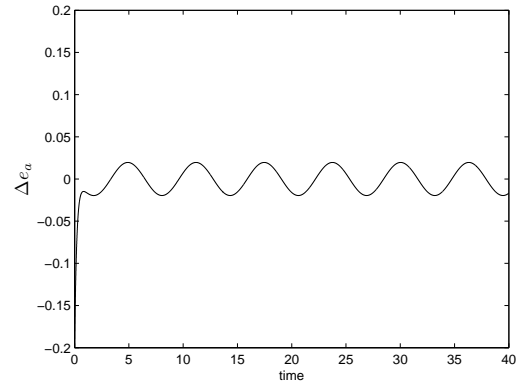
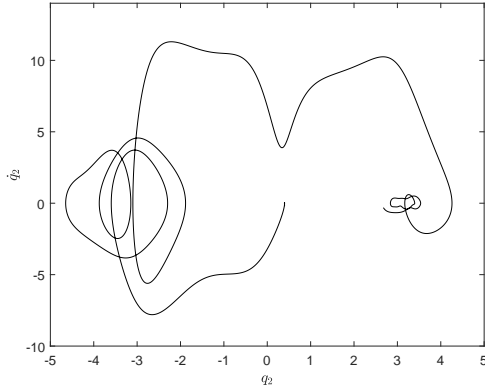
(a) Torque error  $e_a = \tau - \tau^*$ .(b) Deviation  $\Delta e_a = \xi_5 - e_a$  of the torque error from its estimate.

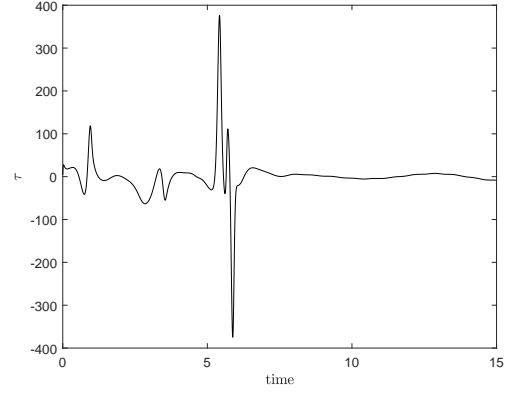
Figure 12.: Torque tracking error and its estimate for the voltage-driven plant in the presence of disturbances.

### 3.3.2 Sensitivity of the torque-based synthesis to structural perturbations

To add practical value to the present investigation, the torque synthesis of the cart-pendulum model (with the same plant-actuator parameters, specified in Table 1 and Table 2) is tested while being coupled to the motor dynamics. In the absence of external disturbances  $w = [w_q^T, w_\tau^T, w_y^T]^T = [w_x, w_\theta, w_\tau, w_{y1}, w_{y2}]^T = [0, 0, 0, 0, 0]^T$ , the actuator dynamics are further viewed as a structural perturbation for the cart-pendulum system. Thus, the control input is designed for the torque-driven cart-pendulum model but it is realistically applied by passing through the motor dynamics. Numerical results for this scheme are given in Figures 13 and 14. Figure 13a depicts the pendulum motion on the  $(q_2, \dot{q}_2)$ -phase portrait projection. Figures 13b shows the torque input, thus designed, to apply unrealistically large values. The tracking error 2-norm and that of its estimate are shown in Figure 14 for the torque-driven cart-pendulum model coupled to the motor dynamics, viewed as a structural perturbation. As concluded from these figures, the structural perturbation destroys the orbital stabilization of the torque-based synthesis. It is thus shown that under certain relations between the plant and motor dynamics (when the latter are not too fast compared to the former), orbital stabilization should involve the voltage synthesis to correctly reproduce the applied torque, otherwise, the orbital stabilization is not accomplished.

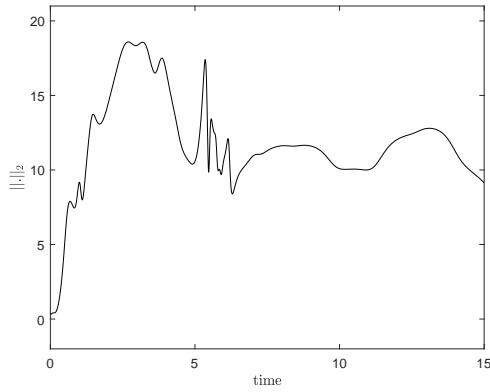


(a) Torque-driven pendulum motion on  $(q_2, \dot{q}_2)$ -plane, affected by actuator dynamics.

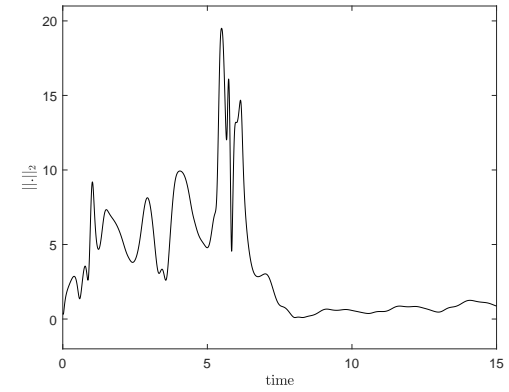


(b) Control input, computed for the torque-driven model and affected by actuator dynamics.

Figure 13.: Sensitivity of the torque-based orbital stabilization to structural perturbations



(a) Tracking error  $\|(e_{p1}, e_{p2}, \dot{e}_{p1}, \dot{e}_{p2})^T\|_2$  for the torque synthesis of the coupled plant-actuator dynamics.



(b) Deviation =  $\|(\xi_1 - e_{p1}, \xi_2 - e_{p2}, \xi_3 - \dot{e}_{p1}, \xi_4 - \dot{e}_{p2})^T\|_2$  of the tracking error from its estimate.

Figure 14.: Performance of the torque-based orbital stabilization to structural perturbations.

#### 4. Conclusions

The generation of periodic motions is constructively addressed for mechanical systems of underactuation degree one, driven by electrical motors with their own dynamics. The VC approach and nonlinear  $\mathcal{H}_\infty$  output feedback synthesis are coupled together in a unified framework to yield the robust orbitally stabilizing synthesis. The developed synthesis is reminiscent of that of MRAC and it is feasible in practice for a wide class of electromechanical systems with incomplete state measurements, operating under external disturbances and measurement noise. Performance issues are illustrated in the numerical study made for a voltage-driven cart-pendulum testbed. Comparison to the reduced order  $\mathcal{H}_\infty$  synthesis, applied to the torque-driven cart-pendulum model where motor dynamics are ignored, reveals benefits of the proposed approach.

## Referencias

- ANDERSON, B.D. AND MOORE, G.B. (1989) *Optimal Control – Linear Quadratic methods*, Englewood Cliffs: Prentice Hall International.
- ANDRONOV, A.A. AND VITT, A. (1933) *On Lyapunov stability*, *Exper. Theor. Phys.*, **3**, 373–374.
- BROGLIATO, B., LOZANO, R., FALK, R.S. & EGELAND, O. (2007) *Dissipative Systems Analysis and Control—theory and Applications*, London: Springer Verlag.
- CHEN, B., UANG, H. & TSENG, C. (1998) Robust tracking enhancement of robot systems including motor dynamics: A fuzzy-based dynamic game approach, *IEEE Transactions on Fuzzy Systems*, **6**(4), 538–552.
- CHEVALLEREAU, C., BESSONNET, G., ABBA G. & AOUSTIN, Y. (2013) *Bipedal robots: Modeling, design and walking synthesis*, John Wiley & Sons.
- COLANERI, P. (2000) Continuous-time periodic systems in  $H_2$  and  $H_\infty$ . Part I: Theoretical aspects, *Kibernetika*, **36**(2), 211–242.
- COLANERI, P. (2000) Continuous-time periodic systems in  $H_2$  and  $H_\infty$ . Part II: State feedback problems, *Kibernetika*, **36**(3), 329–350.
- FOMIN, V.N., FRADKOV A.L. & YAKUBOVICH, V.A. (1981) *Adaptive control of dynamic objects*, Moscow: Nauka.
- FRADKOV A.L., MIROSHNIK I.V. & NIKIFOROV, V.O. (1999) *Nonlinear and adaptive control of complex systems*, Dordrecht: Kluwer.
- FREIDOVICH, L., ROBERTSON, A., SHIRIAEV, A. & JOHANSON, R. (2008) Periodic motions of the Pendubot via virtual holonomic constraints: Theory and experiments, *Automatica*, **44**, 785–791.
- HARTMAN, P. (1964) *Ordinary Differential Equations*, New York: Wiley.
- ISIDORI A. & ASTOLFI A. (1992) Disturbance attenuation and  $\mathcal{H}_\infty$ -control via measurement feedback in nonlinear systems., *Automatic Control, IEEE Transactions on*, **37**(9), 1283–1293.
- LENOV, G. A. (2006) Generalization of the andronov-vitt theorem., *Regular Chaotic Dyn.*, **11**(1), 281–289.
- MOON, J., DOH, T. & CHUNG, M. (1997) An iterative learning control scheme for manipulators, *Proceedings of the 1997 IEEE/RSJ International Conference on Intelligent Robots and Systems IROS'97*, 759–765.
- ORLOV, Y., AGUILAR, L. & ACHO, L. (2005) Model orbit robust stabilization (MORS) of Pendubot with application to swing up control, *Proceedings of the 44th IEEE Conference on Decision and Control/European Control Conference*, 6164–6169.
- ORLOV, Y., & AGUILAR, L.T. (2014) *Advanced  $H_\infty$  Control*, Birkhauser, New York.
- ORTEGA, R., LORIA, A., NICKLASSON, P.J. & SIRA-RAMIREZ, H. (2013) *Passivity-based control of Euler-Lagrange systems: mechanical, electrical and electromechanical applications*, Springer, London
- PHELKIN, S.S., SHIRIAEV, A.S., ROBERTSSON, A., FREIDOVICH, L.B., KOLYUBIN, S.A., PARAMONOV, L.V., & GUSEV, S.V. (2017) On Orbital Stabilization for Industrial Manipulators: Case Study in Evaluating Performances of modified PD+ and Inverse Dynamics Controllers, *IEEE Transaction on Control Systems Tec.*, **25**(1) 101–117.
- RUGH, W. (1996) *Linear System Theory*, 2nd ed. Upper Saddle River, NJ: Prentice-Hall.
- SHIRIAEV, A.S., FREIDOVICH, L.B. & GUSEV, S.V. (2010) Transverse Linearization for Controlled Mechanical Systems With Several Passive Degrees of Freedom, *IEEE Transaction on Automatic Control*, **55**(4) 893–906.
- SHIRIAEV, A.S., FREIDOVICH, L.B. & MANCHESTER, I.R. (2008) Can we make a robot ballerina perform a pirouette? Orbital stabilization of periodic motions of underactuated mechanical systems, *Annual Reviews in Control*, **32** 200–211.
- SHIRIAEV, A.S., PERRAM, J.W. & SANDBERG, A. (2006) Periodic motion planning for virtually constrained Euler Lagrange systems, *Systems and Control Letters*, **55**(11) 900–907.
- SHIRIAEV, A.S., PERRAM, J.W. & CANUDAS-DE-WIT, C. (2005) Constructive tool for orbital

- stabilization of underactuated nonlinear systems: virtual constraints approach, *IEEE Transaction on Automatic Control*, **50**(8) 1164–1176.
- WANG, L., CHAI, T. & ZHAI, L.(2009) Neural-network-based terminal sliding-mode control of robotic manipulators including actuator dynamics, *IEEE Transactions on Industrial Electronics*, **56**(9) 3296–3304.
- WESTERVELT, E.R., GRIZZLE, J.W., CHEVALLEREAU, C., CHOI, J.H. & MORRIS, B.(2007) *Feedback control of dynamic bipedal robot locomotion*, CRC press Boca Raton.
- YAKUBOVICH, V.A.(1986) Linear-quadratic optimization problem and frequency theorem for periodic systems, *Siberian Math. J.*, **27**(4) 181–200.